Weighted Decision Enhanced Phase-Retrieval Receiver with Adaptive Intensity Transformation

Peijian Zhou(1), Meng Xiang* (1), Gai Zhou(1), Jilong Li(1), Jianping Li(1), Songnian Fu(1), Yuwen Qin (1)

(1)Advanced Institute of Photonics Technology, School of Information Engineering, and Guangdong Provincial Key Laboratory of Information Photonics Technology, Guangdong University of Technology, Guangzhou 510006, China. *Corresponding author: meng.xiang@gdut.edu.cn

Abstract：*We report a weighted decision enhanced phase-retrieval receiver with adaptive intensity transformation (WD_AIT_PR). When 56 GBaud 16QAM signals are transmitted over the 80km SSMF, the WD_AIT_PR receiver is verified to outperform other newly-reported counterparts, in terms of convergence speed, steady BER performance, and imperfections tolerance.*

Induction

Low-cost short to medium reach optical fiber transmission systems prefer direct detection to coherent detection using local oscillators [1]. At the same time, the utilization of higher-level complex modulation formats is highly expected even in such direct detection-based systems to comply with increasing demands for higher data transmission rates. In this context, several advanced receiver solutions to reconstruct the complex-valued signal using direct detection measurements were proposed and extensively studied in recently years, such as the Kramers-Kronig (KK) receiver [2], the Stokes vector receiver (SVR) [3], the carrier assisted differential detection receiver (CADD) [4] and the phase-retrieval (PR) receiver [5]. Among those, the PR receiver is quite promising by circumventing the carrier requirement either at the transmitter-side (Tx) or at the receiver-side (Rx).

Generally speaking, the PR receiver recoveries the signal's full field via intensity-only measurements of different projections by running an optimization algorithm, such as the modified Gerchberg-Saxton (MGS) algorithm, iteratively until the numerically reconstructed intensities at all the projection planes match the measurements. However, the PR based on MGS algorithm usually suffers from the slow convergency and stagnant issue [5]. To ensure a faster and better convergency, a PR receiver using symbol-wise GS error for phase reset, denoted as PR_PR, was firstly proposed [6]. Then we proposed a PR receiver with the aid of adaptive intensity transformation (AIT) to further improve the convergency speed and PR accuracy, denoted as PR_AIT. The PR_AIT receiver was verified capable of accurately retrieving the QPSK signal's phase through around 50 iterations [7]. In [8], hard decisions (HD) of the PAM signal are employed before the pilot insertion to enhance the PR performance of the PAM signal after the fiber transmission. Whereas, the HD operation can only be applied after a large number of iterations with better pre-convergency to guarantee the right decisions. In addition, the HD errors inevitably limit the PR performance.

In this paper, we propose a PR receiver employing weighted decisions (WD) based on a compressed sigmoid nonlinear function and AIT, denoted as WD_AIT_PR, with the capability of both fast convergence and high PR accuracy. Compared with other newly-reported phase-retrieval receivers, both the convergence speed and the steady BER performance are significantly improved. In addition, we identify that the proposed WD_AIT_PR receiver is more robust to the receiver imperfections such as the skew and noise imbalance between the two intensity measurements.

Principle of the WD_AIT_PR receiver

The PR receiver generally comprises an optical splitter, a dispersive element, and two single-ended photodiodes (PDs) and Analog-to-Digital converters (ADCs). Generally, the goal of the PR receiver is to reconstruct the signal from two intensity measurements $|s(t)|^2$ and $|d(t)|^2$. $s(t)$ and $d(t)$ are the undispersed signal and dispersed signal, respectively [6]. We set $a(t)=|s(t)|$ and $b(t)=|d(t)|$ for convenience. The solution for the reconstruction of optical field can be represented as a problem of identifying a phase sign $\angle\tilde{s}(t)$ to satisfy the following equation

$$\underset{\angle\tilde{s}(k)}{argmin}\sum_{m=1}^{N}\left(\left|\sum_{k}(a(k)exp(j\angle\tilde{s}(k))\cdot h_D(mT-kT)\right|-b(mT)\right)^2 \quad (1)$$

where $h_D(t)$ is the complex transfer function induced by the use of the dispersive element, T is the symbol duration.

The process of identifying the values of $\angle\tilde{s}(k)$ that minimize the expression in Eq. (1) is realized by the iterative optimization algorithm with several physical constraints. The proposed WD_AIT_PR solution to the above-mentioned iterative optimization problem is shown in Algorithm 1, where h_{CD} represents the CD transfer functions of the fiber transmission. M is the total number of iterations for the PR receiver. N is iteration number in which the WD operation is introduced. h_{RRC} is the root raised cosine (RRC) shaping filter. t'_p is the time slot assigned for pilot symbols x_p . $\otimes$ represents the convolution operation. A random phase ranging from $-\pi$ to π is initialized and the signal phase is updated after every iteration. Within the iteration loop, the measured signal intensity is first powered by a factor of P which is adaptively adjusted with respect to the current iteration by a maximal powering factor R and a decaying factor V [7]. Then, the reconstructed signal is propagated back to the Tx by imposing the CD compensation h_{CD}^{-1} . After passing through an RRC filter and being down-sampled to 1 sample per symbol (Sps), WD is introduced after N times of iterations. Specifically speaking, the WD for the complex-valued signal $\hat{s}(t)$ can be represented as:

$$\hat{s}_{WD}(t) = complex(\hat{s}_{WD}^{I}(t), \hat{s}_{WD}^{Q}(t)) \quad (2)$$

$$\hat{s}_{WD}^{I}(t) = \hat{s}^{I}(t) + f(\gamma^{I}(t)) \cdot E^{I}(t), \quad E^{I}(t) = \hat{s}_{HD}^{I}(t) - \hat{s}^{I}(t) \quad (3)$$

$$\hat{s}_{WD}^{Q}(t) = \hat{s}^{Q}(t) + f(\gamma^{Q}(t)) \cdot E^{Q}(t), E^{Q}(t) = \hat{s}_{HD}^{Q}(t) - \hat{s}^{Q}(t) \quad (4)$$

where $\hat{s}^{I}(t)$ and $\hat{s}^{Q}(t)$ are the in-phase and quadrature of $\hat{s}(t)$, respectively. $\hat{s}_{HD}^{I}(t)$ and $\hat{s}_{HD}^{Q}(t)$ are the HDs of $\hat{s}^{I}(t)$ and $\hat{s}^{Q}(t)$, respectively. $\gamma^{I}(t) = 1 - |E^{I}(t)|$ and $\gamma^{Q}(t) = 1 - |E^{Q}(t)|$ stand for the in-phase and quadrature reliabilities, respectively. $f(\cdot)$ is a compressed sigmoid function to increase the effect of reliability value when it is a high value as well as decrease this effect when it is a low value, which can expressed as

$$f(x) = \frac{1}{2}\left(\frac{1 - exp[-\alpha(x/\beta - 1)]}{1 + exp[-\alpha(x/\beta - 1)]} + 1\right) \quad (5)$$

where α is a positive integer and β with $0 < \beta \le 1$ is a compression factor. Both α and β are required to be optimized to ensure the best performance. Thereafter, the pilot constraint is implemented to update the phase of the samples at the pre-determined locations. Then, the electrical signal is up-sampled to 2 Sps and RRC shaped. After further propagating to the projection plane, the signal intensity is replaced by the transformed intensity. And then the updated signal is propagated to the Rx and the signal phase is correspondingly updated for the next iteration. Please note that the algorithm is implemented in a block-wise manner and the signal propagation and the shaping are processed in the frequency domain.

As we can see, the WD values can be regarded as virtual pilots which are utilized as an extra strong constraint at the Tx without sacrificing the spectral efficiency. As a result, WD enables a faster and better convergency of the iterative PR process. In addition, unlike using HD, the utilization of WD can avoid larger decision errors which in turn benefit for the escape of PR local minimum.

Algorithm 1. WD_AIT_PR algorithm		
Function WD_AIT_PR ($a(t), b(t), R, V, h_{CD}, h_D, M, N$)		
1.	$\angle\hat{s}(t) = \angle rand(t)$	◊ Initialize phase
2.	**For** i **from 1 to** M	
3.	$a(t) \leftarrow a(t)^P$, $b(t) \leftarrow b(t)^P$; $where \;\; P = (R-1) \cdot exp(-i/V) + 1$	◊ AIT
4.	$\hat{s}(t) = a(t) exp(j\angle\hat{s}(t))$	◊ Reconstruct the filed
5.	$\hat{s}(t) \leftarrow h_{CD}^{-1}(t) \otimes \hat{s}(t)$	◊ Propagate back to Tx
6.	$\hat{s}(t) \leftarrow h_{RRC}(t) \otimes \hat{s}(t)$	◊ RRC shaping
7.	$\hat{s}(t') \leftarrow \hat{s}(t)$	◊ Down-sample to 1 Sps
8.	**If** $i > N$ $\hat{s}(t') = complex(\hat{s}_{WD}^{I}(t'), \hat{s}_{WD}^{Q}(t'))$	◊ introduce WD constraint
9.	$\hat{s}(t'_p) \leftarrow \lvert s_p(t'_p) \rvert exp(j\angle s_p(t'_p))$	◊ Pilot constraint
10.	$\hat{s}(t) \leftarrow \hat{s}(t')$	◊ Up-sample to 2 Sps
11.	$\hat{s}(t) \leftarrow h_{RRC}(t) \otimes \hat{s}(t)$	◊ RRC shaping
12.	$\hat{s}(t) \leftarrow h_{CD}(t) \otimes h_D(t) \otimes \hat{s}(t)$	◊ To projection plane
13.	$\hat{s}(t) \leftarrow b(t) exp(j\angle\hat{s}(t))$	◊ Intensity update
14.	$\hat{s}(t) \leftarrow h_D^{-1}(t) \otimes \hat{s}(t)$	◊ Propagate back to Rx
15.	Returns $exp(j\angle\hat{s}(t))$	

Simulations and discussions

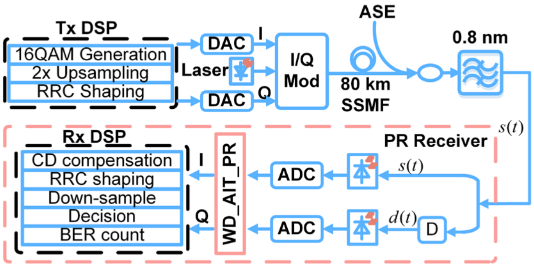

Fig. 1. Simulation setup and DSP flow.

The simulation setup and the corresponding DSP stack are shown in Fig.2. At the Tx DSP, a sequence of 65536 16QAM symbols is first generated with a symbol rate of 56 GBaud. After performing up-sampling, the signal is RRC shaped with a roll-off factor of 0.1. The electrical-to-optical conversion is realized by an In-phase/Quadrature (I/Q) modulator, and a 1550nm Laser with a linewidth of 1 MHz is chosen as the optical carrier. The transmission link consists of a span of 80 km standard single mode fiber (SSMF) with a dispersion parameter of 17 ps/nm/km. After the SSMF transmission, the noise loading module is used to adjust the OSNR of received signals. Thereafter, the signal is fed into the proposed PR receiver, including an optical splitter, a dispersive element with CD of

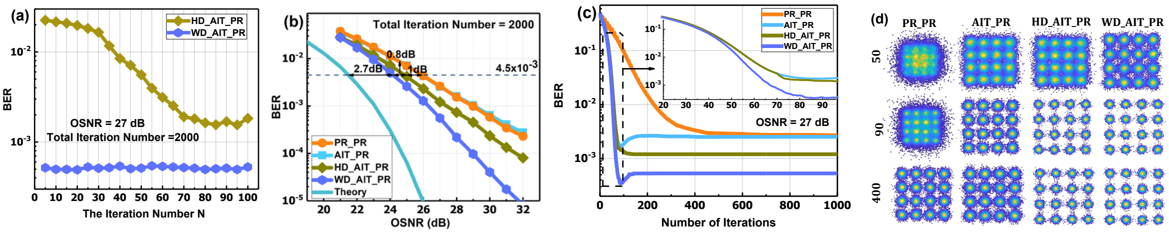

Fig. 2. (a) BER versus the iteration number in which WD/HD starts. (b) BER versus OSNR. (c) BER versus the number of total iterations for PR. (d) The constellation diagrams under various number of iterations.

8500 ps/nm and two single-ended PDs whose response is emulated as a 4th-order Bessel filter with a 3-dB bandwidth of 60 GHz, and two ADCs with a resolution of 6 bits and a sampling rate of 112 GSa/s. Once the signal field reconstruction is realized by using the iterative PR algorithm, the Rx DSP flow including the CD compensation, the matched RRC filtering, the down-sampling to 1 Sps, the symbol decision, and the bit-error-ratio (BER) counting, can be implemented.

Firstly, we investigate the impact of the iteration number N in which WD is introduced in the iteration loop on the PR performance, and the scheme by replacing WD with HD, denoted as HD_AIT_PR, is also taken into account for comparison. The total iteration number is setting at 2000 to ensure a full convergency. As per Fig. 2(a), the WD_AIT_PR scheme is insensitive to N, indicating whenever we begin to implement WD has no impact on the PR performance. However, the performance of the HD_AIT_PR scheme first improves with the increment of N and finally saturates with sufficiently large N. We owe this phenomenon to the fact that HD will introduce large decision errors when HD is applied before the full convergency, and those decision errors will lead to the PR stagnant and degrade the PR performance. To ensure the best performance, N is chosen as 70 and 10 for the HD_AIT_PR and WD_AIT_PR schemes, respectively. In addition, we find the WD_AIT_PR scheme outperforms the HD_AIT_PR scheme as the WD helps to escape the local minima of PR.

Then, we evaluate the BER results with respect to the OSNR after 2000 iterations, as shown in Fig. 2(b). The proposed WD_AIT_PR scheme can significantly reduce the BER, when it's compared with other schemes for various OSNRs. As a result, to reach 7% FEC threshold of BER=4.5$\times$10^{-3} [9], the required OSNR for the proposed WD_AIT_PR scheme can be reduced by 0.8 dB,1.8 dB and1.8 dB in comparison with the HD_AIT_PR, AIT_PR, and PR_PR schemes, respectively.

Next, we investigate the performance of convergence speed and get the relationship between the achieved BER and the number of iterations as shown in Fig. 2(c). The PR_PR scheme shows the worst convergency performance. With the help of AIT, the PR convergency speed can be significantly accelerated. By further using WD, the convergency performance in terms of both convergency speed and steady PR accuracy can be improved. As a result, about 70 iterations are required for the WD_AIT_PR scheme to reach a steady BER around of 4$\times$10^{-4}. The constellation diagrams under different number of iterations are also presented in Fig. 2(d). The WD_AIT_PR scheme always shows the most clear constellation, in comparison with other schemes.

Finally, we investigate the tolerance towards PR receiver imperfections in practical implementations, including the skew and noise imbalance between two tributary signals $s(t)$ and $d(t)$. Note that we load additional noise to the signal $d(t)$ to emulate the noise imbalance, which indeed results in an OSNR difference. Fig. 3 shows the required OSNR penalty to reach 7% FEC threshold with respect to the PR receiver imperfections. As we can see, the proposed WD_AIT_PR scheme shows the best tolerance to the receiver imperfections, especially the skew.

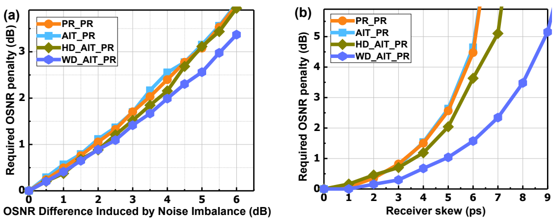

Fig. 3. Tolerance towards (a) OSNR difference and (b) Skew between two tributary signals in the PR receiver.

Conclusion

We have reported a weighted decision enhance PR receiver with adaptive intensity transformation, and numerically reconstructed 56 GBaud 16QAM signals after the 80km SSMF transmission. The proposed PR receiver was verified to show faster convergency speed, lower steady BER performance, and better imperfection tolerance, in comparison with other newly-reported PR receivers.

Acknowledgements

This work is supported by National Key Research and Development Program of China (2018YFB1801001), National Natural Science Foundation of China (62075046, U21A20506).

Reference

[1]. William Shieh, and Honglin Ji. "Advanced Direct Detection Schemes." Optical Fiber Communication Conference. Optical Society of America, 2021.
DOI: 10.1364/OFC.2021.Th4D.5

[2]. Antonio Mecozzi, Cristian Antonelli, and Mark Shtaif, "Kramers–Kronig coherent receiver," Optica. **3**,1220-1227 (2016)
DOI: 10.1364/OPTICA.3.001220

[3]. Di Che, An Li, Xi Chen, Qian Hu, Yifei Wang, and William Shieh, "Stokes Vector Direct Detection for Linear Complex Optical Channels," Journal of Lightwave Technol. **33**, 678-684 (2015)
DOI:10.1109/JLT.2014.2364311

[4]. William Shieh, Chuanbowen Sun and Honglin Ji， "Carrier-assisted differential detection," Light: Science & Applications(2020) 9:18
DOI: 10.1038/s41377-020-0253-8

[5]. Haoshuo Chen, Nicolas K. Fontaine, Joan M. Gene, Roland Ryf, David T. Neilson, and Gregory Raybon, "Dual Polarization Full-Field Signal Waveform Reconstruction Using Intensity Only Measurements for Coherent Communications," Journal of Lightwave Technol. **38**, 2587-2597 (2020)
DOI: 10.1109/JLT.2020.2978052

[6]. Haoshuo Chen, Hanzi Huang, Nicolas K. Fontaine, and Roland Ryf, "Phase retrieval with fast convergence employing parallel alternative projections and phase reset for coherent communications," Optics Letters. **45**, 1188-1191 (2020)
DOI: 10.1364/OL.385435

[7]. Meng Xiang, Peijian Zhou, Bolin Ye, Songnian Fu, Ou Xu, Jianping Li, Di Peng, Yuncai Wang, and Yuwen Qin, "Adaptive intensity transformation-based phase retrieval with high accuracy and fast convergence," Optics Letters. **46**,3215-3218 (2021)
DOI: 10.1364/OL.433349

[8]. Shaohua Hu, Jianming Tang,Jing Zhang,Kun Qiu, "Linearization of Optical IMDD Transmission Systems Using Accelerated Iterative Algorithms," 2020 European Conference on Optical Communications (ECOC), 2020, pp. 1-4,
DOI: 10.1109/ECOC48923.2020.9333139

[9]. Benjamin P. Smith, Arash Farhood, Andrew Hunt, Frank R. Kschischang and John Lodge, "Staircase Codes: FEC for 100 Gb/s OTN," in Journal of Lightwave Technology, vol. 30, no. 1, pp. 110-117, Jan.1, 2012,
DOI: 10.1109/JLT.2011.2175479